

## In Silico and In Vivo Studies of Carboxymethyl Cellulose Based Hydrogels from Cassava Stem and Young Papaya Seed Extract for Diabetic Wounds

Risma Rahmawati<sup>1</sup>, Annisa Firda Lestari<sup>1</sup>, Putri Regita Anggraini<sup>2</sup>, Rahmadita Irma Safitri<sup>3</sup>, Alfi Rizki A'yunin<sup>3</sup>, Maulidan Firdaus<sup>1\*</sup>

<sup>1</sup>Department of Chemistry, Faculty of Mathematics and Natural Sciences, Sebelas Maret University, Surakarta, Jawa Tengah, Indonesia

<sup>2</sup>Department of Biology, Faculty of Mathematics and Natural Sciences, Sebelas Maret University, Surakarta, Jawa Tengah, Indonesia

<sup>3</sup>Department of Pharmacy, Faculty of Mathematics and Natural Sciences, Sebelas Maret University, Surakarta, Jawa Tengah, Indonesia

\*Correspondence author email: maulidan@mipa.uns.ac.id

Received December 22, 2022; Accepted February 22, 2024; Available online July 20, 2024

**ABSTRACT.** Diabetic chronic wound care remains a global challenge due to higher rates of infection leading to amputations and death. The development of wound dressing materials with good biocompatibility, adequate mechanical strength, high absorption, and anti-inflammatory and antibacterial properties are criteria for ideal wound dressings in clinical applications. This study aimed to prepare hydrogel plasters based on carboxymethyl cellulose (CMC) from cassava stems (*Manihot esculenta* C.) with the addition of an active substance from young papaya seeds (*Carica papaya* L.) for diabetic wound healing. The methods used included CMC synthesis, extraction of young papaya seeds, preparation of nanoparticles, hydrogel optimization using Response Surface Methodology (RSM), in silico study, and in vivo tests. All products for each stage were characterized by FTIR and XRD. Hydrogels were characterized by testing pH, organoleptic, swelling ratio, gel fraction, biodegradability, FTIR, and SEM. The results of RSM optimization obtained hydrogel with the formula Na-CMC 3%, citric acid 2%, and stirring temperature 70°C. Based on the in-silico test results, the apigenin compound has the lowest binding energy, namely -9.4 kcal/mol, so it has the potential to heal diabetic wounds by triggering angiogenesis through the VEGFR2 signal. In vivo test results showed that the hydrogel with the addition of young papaya seed extract had the fastest wound healing rate compared to other treatments, marked by 100% wound closure on the 10th day.

**Keywords:** carboxymethyl cellulose, cassava stem, diabetes wound, hydrogel, young papaya seeds.

## INTRODUCTION

Diabetes mellitus (DM) represents a widespread metabolic disorder characterized by elevated blood glucose levels, leading to persistent complications. The global diabetic population, as indicated by the 2021 data from the International Diabetes Federation (IDF), has surged to a staggering 536.6 million, accentuating the heightened risk of associated complications. Among these complications, DM foot wounds show up as the main contributors to amputations and deaths. The susceptibility of DM wounds against bacterial infections, particularly by the typical pathogen *Streptococcus aureus* (*S. aureus*), leads to a considerable problem in the healing progression (Lavigne et al., 2021). Wound dressings show a vital contribution in mitigating infections in DM wounds. Hydrogels, because of their elasticity and biocompatibility, have acquired consideration as potential candidates for ideal wound dressings.

Hydrogels consist three-dimensional (3D) hydrophilic matrix that demonstrates water-swelling

abilities though remaining insoluble, providing an ideal environment for wound care. Their characteristics, mimicking the extracellular matrix (ECM), comprise strong swelling capacities advancing considerable exudate absorption and high hydrogel porosity, thus allowing effective oxygen transmission inside wound tissues (Zhang et al., 2021). Dissimilar from other wound dressing possibilities, hydrogels are attaining extensive recognition as a crucial solution for tissue restoration because of their natural ECM-mirroring structure through adjustable properties (Zeng et al., 2022; Qi et al., 2022). These polymeric materials have prominent 3D matrix structures with hydrophilic macromolecular chains, efficiently absorbing and holding significant water volumes in their interstitial structures (Parani et al., 2016; Kabir et al., 2018). Hydrogels, characterized by excellent wound exudate penetrable properties, hydrophilicity, moisture-retention ability, and oxygen permeability, are approved as very promising wound dressings having the ability to adapt to irregular wounds (Capanema et al. 2023).

Hydrogels from natural polysaccharide derivates, such as carboxymethyl cellulose (CMC), have gained attention due to their environmentally benign, biocompatible, and biodegradable characteristics (Parid et al., 2018). CMC shows effectiveness in hydrogel synthesis, offering a renewable and non-toxic choice. An interesting potency lies in using cassava stems, an agricultural byproduct consisting of 56.82%  $\alpha$ -cellulose (Widiarto et al., 2019), for CMC synthesis. In spite of the considerable cassava production in Indonesia (19 MT in 2018), the possible utilization of cassava stems remains mostly uninvestigated. In this research, cellulose isolated from cassava stems takes the midpoint point as an essential constituent in the preparation of hydrogel plasters.

Only relying on hydrogel dressings is not adequate to heal DM wounds, and thus active constituents need to be included in inhibiting the growth of bacteria. One active substance that has the possibility of inhibiting the growth of bacteria is papaya (*Carica papaya* L.) seeds. Papaya seeds have not been extensively utilized although, in 2020, the total papaya production in Indonesia reached 1 MT (BPS, 2020). Papaya seeds consist of flavonoids, tannins, saponins, alkaloids, and phenolics that can be used as antibacterial agents (Kong et al., 2021). Previous study shows that the ethanol extract in young/unripe papaya seeds has greater antibacterial activity than old papaya seeds against the growth of *S. aureus* bacteria (Mulyono, 2013). In addition, young/unripe papaya seeds contain the derivatives of flavonoid and phenolic, such as quercetin, kaempferol, apigenin, caffeic acid, ferulic acid, and chlorogenic acid, which act to induce angiogenesis via VEGFR2 signaling and can accelerate DM wound healing (Singh et al., 2020).

In the realm of hydrogel research, diverse research has explored the utilization of cellulose derivatives from various starting materials, as demonstrated by studies incorporating materials i.e. rice husks (Wan Ishak et al., 2018), pineapple leaves (Tuyet Phan et al., 2021), corn cobs (Enawgaw et al., 2021) and bamboo (Cao et al., 2022). Nevertheless, an obvious void exists in the scientific literature relating to hydrogels, which are methodically derived from cassava stem cellulose in combination with the incorporation of bioactive compounds from young papaya seeds. This gap in previous research not only features an unexplored method in the formulation of hydrogel but also highlights the unique and advanced nature of the present study. Therefore, this study focuses on the development of hydrogel plasters that involve the combination of cellulose from cassava stems and active substituents derived from young papaya seeds. This study is thoroughly substantiated over comprehensive assessments using both in silico computation and in vivo evaluations, thus contributing characteristic understandings in the field of biomaterials and wound care inventions.

## EXPERIMENTAL SECTION

### Materials

The materials employed in this research involved several components to prepare the extract, hydrogel preparation, in vivo evaluation, and in-silico simulations. For the extract and hydrogel preparations, young papaya seeds, cassava stems, and all commercial products purchased from Merck i.e. NaOH,  $C_2H_5OH$  96%,  $CH_3OH$ ,  $CH_3COOH$  glacial,  $NaOCl_2$ , sodium chloroacetate ( $CH_2ClCO_2Na$ , SCA), citric acid, chitosan, and NaTPP were used. The in vivo studies included the use of BALB/c mice, ketamine, and alloxan (Sigma Aldrich). Furthermore, resources for the in-silico simulations involved apigenin (CID: 5280443), quercetin (CID: 5280343), chlorogenic acid (CID: 1794427), kaempferol (CID: 5280863), and caffeic acid (CID: 689043). Furthermore, a macromolecule, characterized in the form of protein VEGFR2 (PDB ID: 3VHE), was used in the in-silico simulations.

### Equipment

The Fourier Transform Infrared (FTIR) spectra were recorded from the Shimadzu Prestige-21 spectrophotometer. The particle size distribution and zeta potential value were measured using Particle Size Analyzer (PSA, Malvern Panalytical) and Zetasizer (NanoZS), respectively. The morphology of the hydrogel was scanned using Scanning Electron Microscopy (SEM, Quanta 250). The X-ray diffraction (XRD) measurement was performed using an XRD D8 Advance Bruker, Germany. The in-silico experiment was done using various software, such as Autodock vina, AutoDock ver. 1.5.7, Pymol ver. 2.5.2, OpenBabel, Avogadro, and Discovery Studio 2021 Client. Relevant data was extracted from the Pubchem and Uniprot databases and then used to improve the in-silico simulation.

### Preparation of Young Papaya Seed Nanoparticle Extract

The nanoparticle extract of young papaya seed was prepared by maceration of 100 g of the dried seed powder with 800 mL of 96% ethanol for 3 days. The solvent was replaced every day. The macerated extract was filtered and concentrated over a rotary evaporator. An amount of 1 g of the extract was diluted in 35 mL of ethanol and stirred with the addition of 15 mL of distilled water. A total of 1 g of chitosan was dissolved in 100 mL of 1% glacial acetic acid. Then a NaTPP solution was also prepared by dissolving 1 g of NaTPP in 100 mL of distilled water. In equimolar ratio, chitosan, extract, and NaTPP were mixed and stirred for 1.5 hours. The obtained extract was subjected to a phytochemical test and analyzed using the PSA and Zetasizer.

### Isolation of $\alpha$ -cellulose

The isolation started by bleaching 10 g cassava stem fiber was carried out using 200 mL sodium hypochlorite (2.5%) and acetic acid was added until

the pH value reached 4. The fiber was heated at 70 °C for 2 h. The fiber was separated and washed with distilled water, then dried at 55 °C for 16 h. The result was then alkalinized using 18% (w/v) NaOH by maintaining a fiber-to-NaOH ratio of 1:23 (g/mL) for 2.5 h. at room temperature. The mixture was filtered, washed, and dried in an oven at 55 °C for 1 day. The obtained fibers were characterized using FTIR and XRD.

### Synthesis of Na-CMC

The isolated  $\alpha$ -Cellulose (10 g) was alkalinized using a mixture of 100 mL isopropyl alcohol and 15 mL of 25% (v/v) NaOH at room temperature for 1.5 h. To perform carboxymethylation, the mixture was then reacted with 7 g of SCA at 50 °C for 3 h. The result was filtered and soaked in 250 mL methanol for 17 h. Neutralization was then performed using  $\text{CH}_3\text{COOH}$ . The neutral mixture was then filtered and washed with ethanol. The residue was dried at 55 °C for 1 day and characterized using FTIR and XRD.

### Hydrogel Preparation

Na-CMC with varying concentrations of 4% (w/v) was dissolved in distilled water and stirred using a magnetic stirrer for 24 hours at room temperature. When the mixture became homogeneous, citric acid dissolved in 3% (w/v) distilled water was added. After that, stirring was carried out for 1.5 hours at 75 °C. Furthermore, young papaya seed extract nanoparticles were added to the mixture and stirred again for 1 hour. The hydrogel was molded using an 8 × 8 cm glass mold and dried in an oven at 45 °C for 24 hours.

### Hydrogel Characterization

Hydrogel characterizations performed in this research included pH, organoleptic, swelling ratio, gel fraction, FTIR, and SEM. pH paper was used to determine the acidity of the hydrogel. Various organoleptic tests i.e. color, smell, and shape were performed on the hydrogel plasters. The swelling ratio was determined by dipping the hydrogel in distilled water for 20 minutes. The gel fraction was measured by immersing the hydrogel in 96% ethanol for 14 h. Also, to identify the functional groups and to observe the surface morphology of the hydrogel of the hydrogel, FTIR and SEM analyses were respectively carried out. (Dembek et al., 2022).

### Preparation of Bacterial Suspension

Nutrient agar (0.504 g) was dissolved in 18 mL of distilled  $\text{H}_2\text{O}$  and then heated. The medium was placed in three test tubes, each holding up to 5 mL, and sterilized in an autoclave. The tube was tilted and allowed to solidify before being incubated at 37 °C for 24 h. Some loop needles of *S. aureus* bacterial stock were inoculated on the slanting agar and incubated again. The bacteria were put in a test tube containing 2 mL of 0.9% NaCl and compared with a 0.5 McFarland standard solution made from a mixture of 1%  $\text{H}_2\text{SO}_4$  9.95 mL and 1%  $\text{BaCl}_2$  0.05 mL then shaken

until a cloudy solution was formed (Mofrad et al., 2018).

### In Vivo Test

The mice were fasted for 6 hours, then the initial glucose levels were checked by taking blood from the tail. Mice with normal sugar levels were injected intraperitoneally with alloxan as much as 0.3 mg/head and adapted. After the mice had DM, an incision was made on the back of the mice of about 1 × 1 cm with a wound depth of 0.1 cm subcutaneously (Zebua et al., 2021). *S. aureus* bacterial suspension (2  $\mu\text{L}$ ) was dripped on the wound surface. Mice were treated with 5 mice each, namely P1: commercial plaster, P2: hydrogel plaster with extract, P3: hydrogel plaster without extract, and P4: no treatment. Observation of the wound was carried out for 10 days.

### In Silico Test

In silico investigations involved ligand optimization and preparation through AutoDock Tools. The target compound underwent analysis based on the Lipinski Rule of Five, utilizing AdmetSAR 2 (Lipinski et al., 2012; Kusumaningsih et al., 2021). Preparation of the target protein involved AutoDock, with the addition of hydrogen atoms and charges. Subsequently, the docking outcomes underwent validation through RMSD value calculations using Pymol (Prasetyo et al., 2023).

## RESULTS AND DISCUSSION

### Young Papaya Seed Extraction

Maceration of young papaya seed extract produced thick brownish extract in 14.75% yield. Phytochemical screening of the seed extract revealed the presence of secondary metabolites such as alkaloids, tannins, flavonoids, and saponins (Table 1). Notably, these results highlight the presence of diverse bioactive components and reveal the potency of hydrogel application.

### Preparation of Bacterial Suspension

*S. aureus* bacteria is one of the infective bacteria that is the main cause of wound infection in diabetes, delaying wound healing and causing inflammation and chronic infection. McFarland's standard solution was used to standardize the number of bacteria in liquid suspensions by comparing the turbidity of the test suspensions. After comparing the turbidity level between the standard solution and the bacterial suspension, almost the same turbidity results were obtained. Based on the turbidity level, the estimated amount of bacterial suspension was  $1.6 \times 10^8$  CFU/mL.

### Particle Size Analyzer and Zetasizer Test

Particle size distribution was performed to determine the sizes of the papaya seed extract. The prepared extract has a distribution of particles with a size of 323.7 nm and a polydispersity index (PDI) value of 0.606 (Figure 1a). Thus, the size of the extract encounters the standards as nanoparticles in the size

**Table 1.** The phytochemical test result of the ethanol extract of young papaya seeds

| Screening | Reagent           | Results                     | Label |
|-----------|-------------------|-----------------------------|-------|
| Alkaloid  | Dragendorff       | An orange stain is formed   | +     |
| Tannin    | FeCl <sub>3</sub> | The black-blue color formed | +     |
| Flavonoid | NaOH              | Yellow color formed         | +     |
| Saponin   | Aquadest          | Foam appears                | +     |

Note: (+) = contains the tested compound

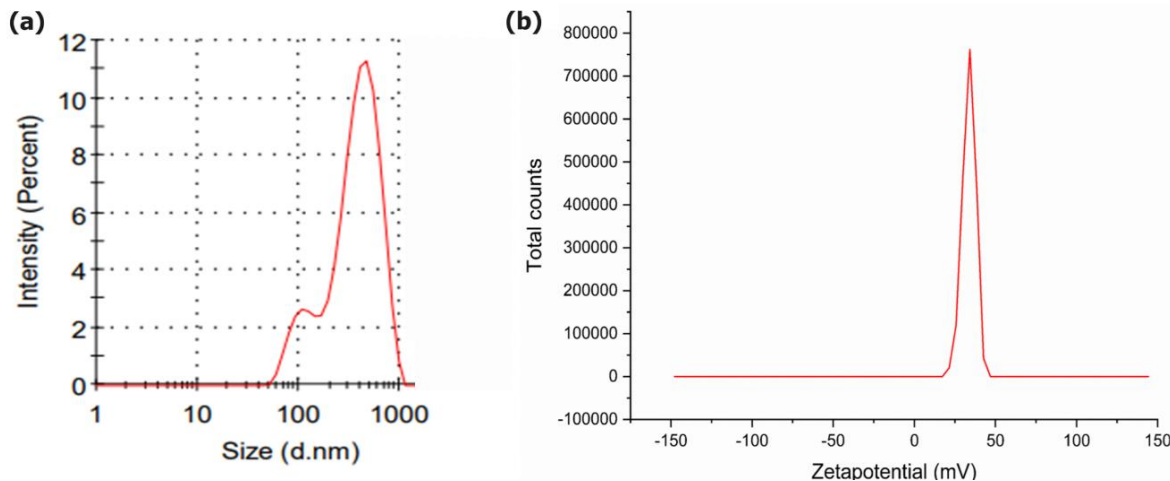


**Figure 1.** PSA (a) and zetasizer result (b) of papaya seed extract

range of 10-10<sup>3</sup> nm and the PDI value ranging from 0.1 to 0.8 indicated that the level of homogeneity of the extract was excellent (Kartini et al., 2020).

The zeta potential value is commonly used to determine the particle charge's nature and the nanoparticles' stability. Based on the measurement results (Figure 1b), a zeta potential value of +33.7 mV was obtained. The positive zeta potential value is due to the contribution of the partial charge on the surface, which is dominated by chitosan (positively charged). In contrast, the zeta potential value > 30 indicates a greater repulsion than attraction to increase the dispersion system's stability. This shows that the sample has high stability.

#### Characterization of $\alpha$ -cellulose and Na-CMC

Carboxymethylation of  $\alpha$ -cellulose using SCA gave white Na-CMC in 18.87% yield. Furthermore, to determine the success of  $\alpha$ -cellulose isolation and synthesis of Na-CMC, FTIR tests were carried out. Based on the results of the FTIR test (Figure 2), it showed that the specific functional groups of  $\alpha$ -cellulose had a peak of 3446 cm<sup>-1</sup>, namely the O-H group, the C-H group at 2894 cm<sup>-1</sup>, and the C-O-C group at 1158 cm<sup>-1</sup>. FTIR test of Na-CMC also showed O-H groups at 3283 cm<sup>-1</sup>, C-H groups at 2894 cm<sup>-1</sup>, and C-O-C groups at 1114 cm<sup>-1</sup>. The results of the Na-CMC spectra showed a peak at 1600 cm<sup>-1</sup> and 1416 cm<sup>-1</sup> which indicated the presence of a carboxymethyl group (Wahyuni et al., 2019).

Based on the diffractogram analysis (Figure 3) showed characteristics of  $\alpha$ -cellulose peaks at 20 of 11.75°, 20.09°, and 21.57° with a crystallinity index of 45.61%. These corresponding peaks are in agreement

with the reported study (El-Sakhaway et al., 2018; Yao et al., 2020). In the case of the Na-CMC, diffractogram analysis displayed peaks at 20 of 19.63° and 31.40° with a crystallinity index of 38.07%. Those peaks are characteristics for Na-CMC which have similar patterns as reported by Kumar et al. (2020).

#### Hydrogel Preparation and Characterization

The hydrogel preparation was optimized by Response Surface Methodology (RSM). RSM has been chosen not only to reveal the output parameters (responses) that are determined by the input process parameters but also to quantify the connection between the variable input parameters and the corresponding output parameters (Prasetyo et al., 2019). RSM is used to optimize the value of the independent variable to achieve the optimal value of the response variable. This method is utilized to reduce experimentation costs and time while ensuring that all possible combinations of independent variables are tested effectively (Kusumaningsih et al., 2020; Istiqomah et al., 2022, Firdaus et al., 2023). In this research, the RSM (Figure 4) was carried out using the Box Behnken Design method with swelling ratio and gel fraction as the responses and the amount of Na-CMC, citric acid, and stirring temperature as the independent variables. Thus, the hydrogel plasters were obtained with the optimum formula of 2% Na-CMC, 3% citric acid, and a stirring temperature of 70 °C. The ANOVA test results confirmed the significance of the model, showed by p-values < 0.05, remarkably 0.0049 and 0.0169 for the swelling ratio and the gel fraction response, respectively.

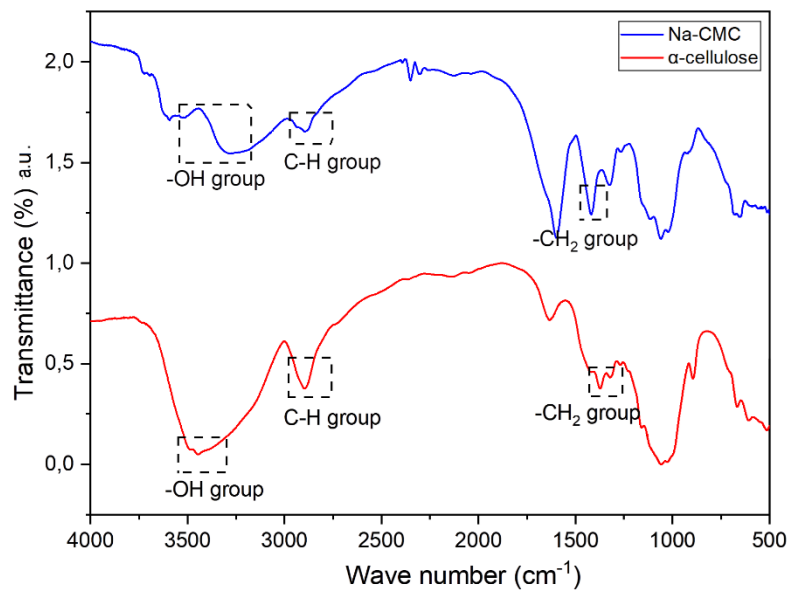


Figure 2. FTIR Spectra of  $\alpha$ -cellulose and Na-CMC (KBr pellet)

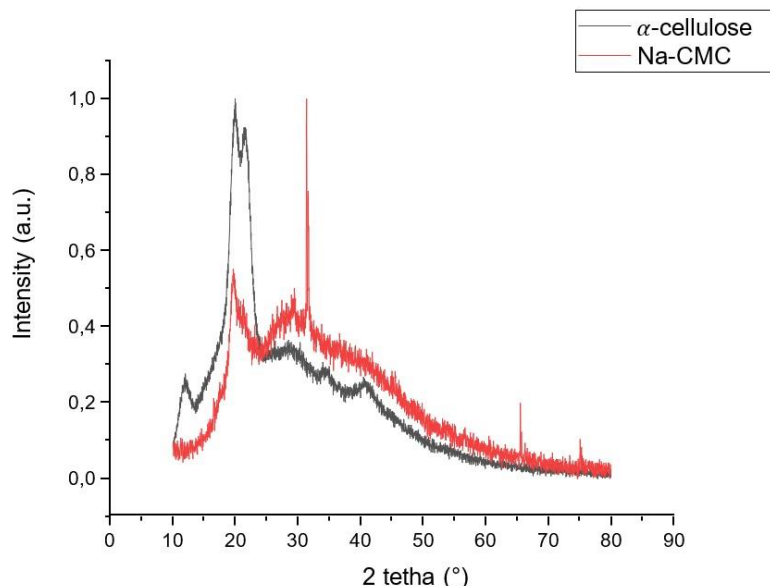


Figure 3. XRD pattern of  $\alpha$ -cellulose and Na-CMC

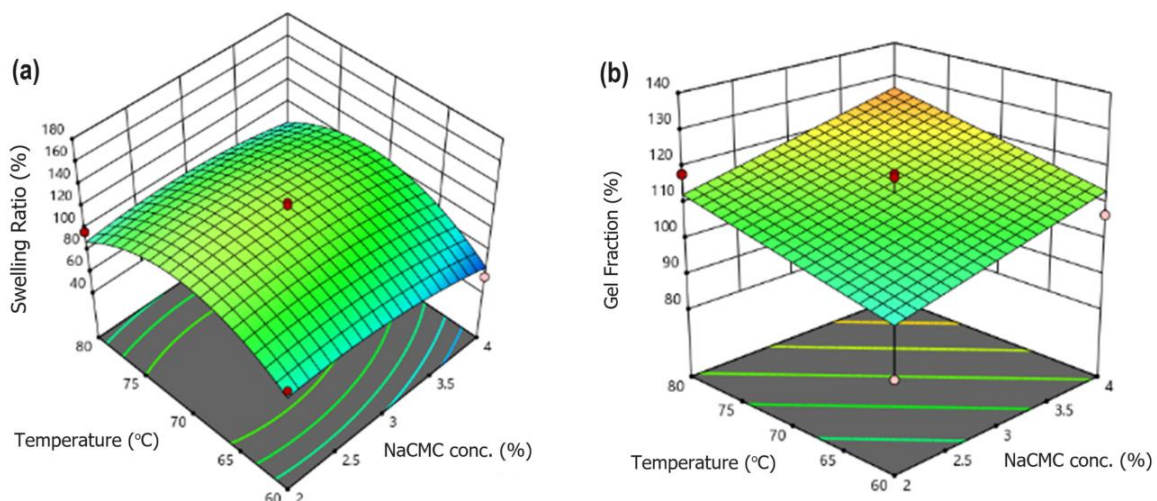
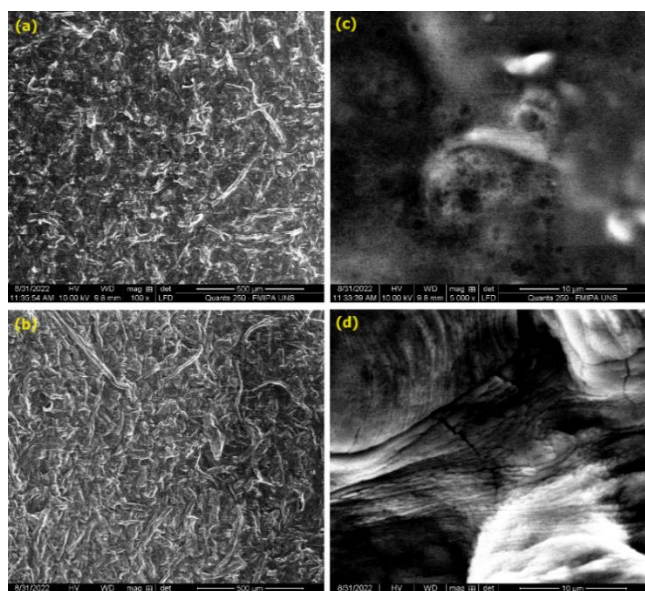


Figure 4. RSM contour of independent variables on the response: (a) Swelling Ratio and (b) Gel Fraction

The hydrogel plaster was obtained in sheet form, exhibiting a clear yellowish color and a slightly sour aroma. The pH of the hydrogel was measured and found to be 4.5. This pH value aligns with the natural pH range of human skin, which typically falls between 4.5 and 7. To assess the water absorption capacity, the synthesized hydrogel underwent swelling ratio testing. The procedure involved immersing the hydrogel in distilled water and measuring its weight before and after immersion. The swelling ratio test yielded a value of 119.075%, indicating the extent to which the hydrogel can absorb water. The gel fraction test, which quantifies the proportion of the hydrogel that remains undissolved, resulted in a value of 129.205%. This high gel fraction suggests the presence of cross-links within the hydrogel structure. The biodegradability test results on the hydrogel plaster produced showed a mass loss of 76.53%, while the commercial plaster had a mass loss of 16.868%.

This indicates that the cassava stem-based Na-CMC hydrogel plaster is more environmentally friendly.

SEM imaging (**Figure 5**) revealed the surface morphology of the hydrogel. Notably, the surface appeared porous, consistent with the cross-linked structure. At 100x magnification, the plaster containing the young papaya seed extract exhibited a clearer and wider porous surface compared to the extract-free plaster. This observation strongly suggests the incorporation of active compounds from the papaya seed extract. Comprehensive characterization of the resulting hydrogels was conducted using FTIR spectroscopy. The FTIR analysis, as illustrated in Figure 6, revealed distinct absorption peaks at 1729 and 1723  $\text{cm}^{-1}$ , corresponding to the C=O ester group. This result shows the successful esterification reaction incorporating the carboxyl group of citric acid and the -OH of cellulose, as described in the study performed by <sup>1</sup>Singh et al. (2020).



**Figure 5.** SEM imaging of hydrogel: without extract (a) and with extract (b), both viewed at 100x magnifications; without extract (c) and with extract, both viewed under 5000x magnifications

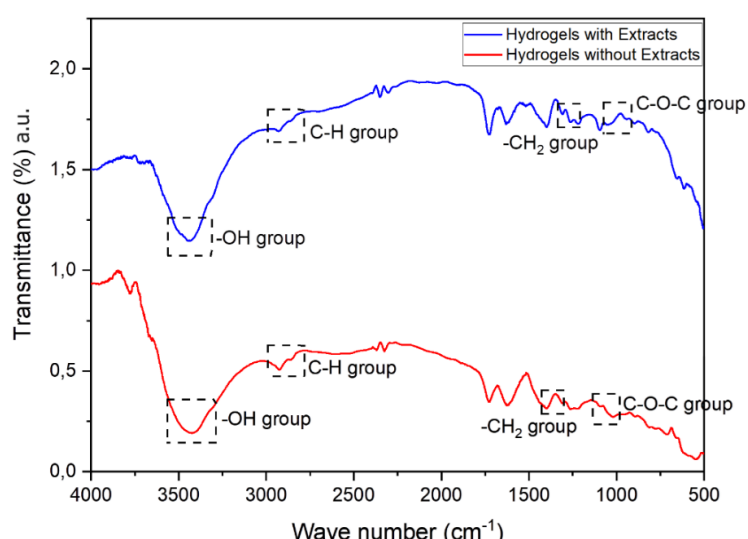


**Figure 6.** FTIR test results of hydrogels without and with extracts

### In Silico Test

The metabolic profile of papaya leaves and seeds with the aim of obtaining information about their phytomedical content has been reported using the metabolite fingerprinting technique (Gogna et al., 2015). Thus, several flavonoids such as naringenin, hesperidin, rutin, kaempferol, and apigenin have reportedly been found in papaya seeds. Additionally, Gogna et al. (2015) also reported that the seed of papaya constitutes phenylpropanoids such as cinnamic acid, coumaric acid, caffeic acid, protocatechuic acid, and chlorogenic acid. According to a study reported by Gazwi et al. (2023), High Performance Liquid Chromatography (HPLC) analysis of papaya seeds exposed the occurrence of ten polyphenol compounds, with quercetin, apigenin, and catechin recognized as major flavonoids, together with pyrogallol, ellagic, and gallic acid as predominant phenolic acids. Information regarding primary and secondary metabolites, as well as active compounds such as alkaloids, flavonoids, and terpenoids is possible to be utilized for grouping medicinal plants. The metabolomic approach provides detailed constituent distribution information, generating a characteristic "metabolic fingerprint" for individual species. Both methods counterpart each other, with chemotaxonomy concentrating on specific compounds and metabolomic fingerprinting providing a comprehensive outline of a plant's whole metabolite profile (Sofrenić et al., 2023). Thus, the active compounds reported by Gogna et al. (2015) and Gazni (2023), such as caffeic acid, chlorogenic acid, kaempferol, quercetin, and apigenin, were then studied over molecular docking.

According to the results of the "Lipinski Rule of Five (RO5)" (Table 2), it can be highlighted that caffeic acid, kaempferol, quercetin, and apigenin fulfill the rules, whereas chlorogenic acid violates one of the RO5 rules, for example, more than 5 hydrogen bond donors. Compounds that violate fewer than two of the five Lipinski rules can still be considered drugs, and thus have the potential to be used as alternative

materials in DM wound healing. Skin sensitization is key in complex immune-mediated skin inflammatory reactions called contact allergic skin infections. These five compounds show negative skin sensitization, so they are safe when applied to the skin.

The outcomes of the molecular docking analysis for bioactive compounds in young papaya seeds revealed that apigenin displayed the highest potential for strong binding with the VEGFR2 protein, evidenced by its remarkably low binding energy of -9.4 kcal/mol (Table 3). The diminished binding energy indicates a robust and stable interaction between the ligand and the target protein. A lower binding energy correlates with heightened affinity, thus signifying the potential of apigenin as a promising compound for the therapeutic management of DM wounds (Verma et al., 2021).

The 3D and 2D visualizations (Figure 7) of the molecular interactions among apigenin and VEGFR2 protein exposed the predominant participation of hydrogen bonds and hydrophobic interactions. The nature of these interactions plays an essential role in influencing the magnitude of binding free energy and the overall stability of the ligand-receptor interaction (Yao et al., 2018). Notably, during the docking process, hydrogen bonds were identified between apigenin and VEGFR2, specifically forming with the amino acid residues ASP A:1046 and LYS A:868. The abundance of  $\pi$ - $\sigma$  interactions, particularly those involving charge transfer, may facilitate the intercalation of compounds within receptor binding sites or target proteins (Arthur and Uzairu, 2019). Molecular docking results also highlighted similarities in amino acid residues between the docking compounds and native ligands, specifically in ASP A:1046, LYS A:868, VAL A:916, LEU A:1035, VAL A:848, VAL A:899, ALA A:866, and LEU A:840. With an equivalent number of amino acid residues, apigenin in young papaya seeds exhibits potential binding to VEGFR2, triggering the angiogenesis process and promoting the formation of new blood vessels a crucial factor in facilitating the healing of DM wounds.

**Table 2.** Ligand parameters to comply with the lipinski rule of five and skin sensitization

| Compound         | Molecular weight | H-bond donors | H-bond acceptors | logP  | Molar refractivity | Skin sensitization |
|------------------|------------------|---------------|------------------|-------|--------------------|--------------------|
| Caffeic acid     | 180.16           | 3             | 3                | 1.20  | 47.16              | No                 |
| Chlorogenic acid | 354.31           | 6             | 8                | -0.65 | 83.50              | No                 |
| Kaempferol       | 286.24           | 4             | 6                | 2.28  | 76.01              | No                 |
| Quercetin        | 302.24           | 5             | 7                | 1.99  | 78.03              | No                 |
| Apigenin         | 270.24           | 3             | 5                | 2.58  | 73.99              | No                 |

**Table 3.** Docking results of bioactive compounds with VEGFR2 protein

| Compound         | Bond Energy (kcal/mol) |
|------------------|------------------------|
| Caffeic acid     | - 7,3                  |
| Chlorogenic acid | - 7,6                  |
| Kaempferol       | - 7,9                  |
| Quercetin        | - 8,1                  |
| Apigenin         | - 9,4                  |

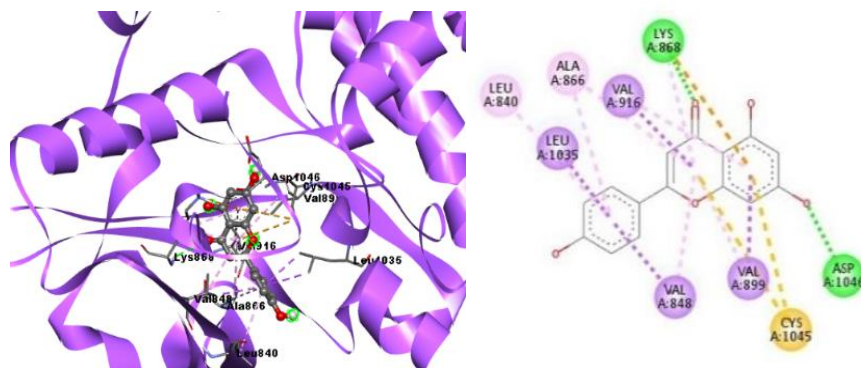


Figure 7. 3D and 2D visualization of docking results

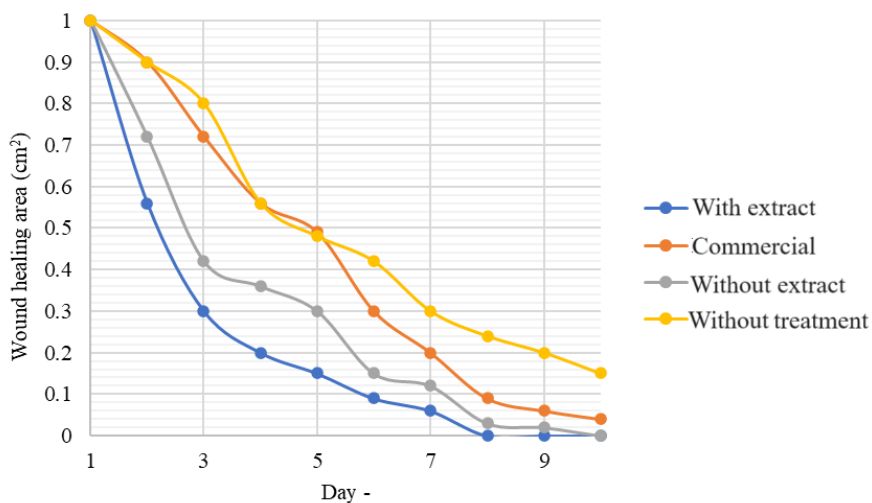


Figure 8. Development of mice wounds over 10 days



Figure 9. Observation of mice wound with extract added-hydrogel plaster treatment

### In Vivo Test

In vivo experiments were conducted using male BALB/c mice with a weight range of 30-40 g. DM was induced in the mice via intraperitoneal administration of alloxan, and blood glucose levels were assessed after a 3-day period, revealing an average blood sugar concentration of 230 mg/dL. As referenced by Yu et al. (2020), normal blood glucose levels in mice typically hover around 100 mg/dL, signifying the successful induction of DM in the experimental mice. Following the onset of DM, the mice underwent depilation, and wounds were carefully created on their dorsal areas. Subsequently, the mice were treated with the designated hydrogel plaster according to the prescribed treatment protocol. The progression of wound development in mice is visually presented in

**Figures 8 and 9.** The experimental findings unequivocally demonstrate superior wound healing efficacy associated with the hydrogel plaster incorporating the extract when compared to the other three treatment groups over the course of the 10-day observation period. Notably, by the 10th day, the wounds treated with the hydrogel plaster containing the extract exhibited complete closure, indicating a remarkable acceleration in the DM wound healing process attributed to the specific bioactive components present in the extract-infused hydrogel. This robust closure outcome on the 10th day underscores the potential therapeutic impact of the formulated hydrogel, suggesting its efficacy in promoting accelerated and comprehensive wound closure, a pivotal milestone in the DM wound healing trajectory.

## CONCLUSIONS

In summary, based on RSM optimization, hydrogel plasters from cassava stems and papaya seeds were successfully synthesized using a formula of 2% Na-CMC, 3% citric acid, and a stirring temperature of 70 °C. The results of the in vivo test showed that hydrogel plasters from cassava stems and young papaya seed extract were effective in inhibiting *S. aureus* bacteria and healing DM wounds which were marked by wound closure on the 10th day. The results of the in-silico test showed that the apigenin compound in young papaya seeds was the compound that had the most potential as a DM wound medicine against the VEGFR2 protein because it had the most negative  $\Delta G$  of -9.4 kcal/mol.

## ACKNOWLEDGMENTS

We extend our deepest appreciation to the Ministry of Education, Culture, Research, and Technology for their generous financial support in funding the 2022 PKM-RE activities, which have made our research endeavors possible.

## REFERENCE

Arthur, D. E., & Uzairu, A. (2019). Molecular docking studies on the interaction of NCI anticancer analogues with human Phosphatidylinositol 4, 5-bisphosphate 3-kinase catalytic subunit. *Journal of King Saud University-Science*, 31(4), 1151-1166. <https://doi.org/10.1016/j.jksus.2019.01.011>

Badan Pusat Statistik (BPS). (2020). *Produksi tanaman buah-buahan 2020*. Retrieved from Badan Pusat Statistik (bps.go.id). Accessed 14 Feb 14, 2022.

Capanema, N. S. V., Mansur, A. A. P., Carvalho, I. C., Carvalho, S. M., & Mansur, H. S. (2023). Bioengineered water-responsive carboxymethyl cellulose/poly (vinyl alcohol) hydrogel hybrids for wound dressing and skin tissue engineering applications. *Gels*, 9(2), 166. <https://doi.org/10.3390/gels9020166>.

Cao, X., Li, F., Zheng, T., Li, G., Wang, W., Li, Y., Chen, S., Li, X., & Lu, Y. (2022). Cellulose-based functional hydrogels derived from bamboo for product design. *Frontiers in Plant Science*, 13, 958066. <https://doi.org/10.3389/fpls.2022.958066>.

Dembek, M., Bocian, S., & Buszewski, B. (2022). Solvent influence on zeta potential of stationary phase—mobile phase interface. *Molecules*, 27(3), 968. <https://doi.org/10.3390/molecules27030968>.

El-Sakhawy, M., Kamel, S., Salama, A., & Tohamy, H. A. S. (2018). Preparation and infrared study of cellulose base damphiphilic materials. *Cellulose Chemistry and Technology*, 52(3-4), 193-200.

Enawgaw, H., Tesfaye, T., Yilma, K. T., & Limeneh, D. Y. (2021). Synthesis of a Cellulose-Co-AMPS Hydrogel for Personal Hygiene Applications Using Cellulose Extracted from Corncobs. *Gels*, 7(4), 236. <https://doi.org/10.3390/gels7040236>.

Firdaus, M., Alawiyah, N., Pratama, J. H., Yaqin, A. N., Handayani, I., & Wibowo, F. R. (2023). Coating based on cellulose from oil palm empty fruit bunches and chitosan doped by Ag+: multivariate optimization and DFT analysis. *New Journal of Chemistry*, 47(34), 16197-16205. <https://doi.org/10.1039/D3NJ01988H>.

Gogna, N., Hamid, N., & Dorai, K. (2015). Metabolomic profiling of the phytomedicinal constituents of *Carica papaya* L. leaves and seeds by <sup>1</sup>H NMR spectroscopy and multivariate statistical analysis. *Journal of Pharmaceutical and Biomedical Analysis*, 115, 74-85. <https://doi.org/10.1016/j.jpba.2015.06.035>.

Gazwi, H. S., Soltan, O. I., & Abdel-Hameed, S. M. (2023). Cakes fortified with papaya seeds effectively protects against CCl<sub>4</sub>-induced immunotoxicity. *Environmental Science and Pollution Research*, 30, 111511-111524. <https://doi.org/10.1007/s11356-023-30172-w>.

International Diabetes Federation. (2021). *IDF diabetes atlas 10th edition*. Retrieved from [https://diabetesatlas.org/data/en/country/94/i\\_d.html](https://diabetesatlas.org/data/en/country/94/i_d.html). Accessed Sept 4, 2022.

Istiqomah, A., Utami, M. R., Firdaus, M., Suryanti, V., & Kusumaningsih, T. (2022). Antibacterial chitosan-Dioscorea alata starch film enriched with essential oils optimally prepared by following response surface methodology. *Food Bioscience*, 46, 101603. <https://doi.org/10.1016/j.fbio.2022.101603>.

Kabir, S. F., Sikdar, P. P., Haque, B., Bhuiyan, M. R., Ali, A., & Islam, M. N. (2018). Cellulose-based hydrogel materials: Chemistry, properties and their prospective applications. *Progress in Biomaterials*, 7, 153-174. <https://doi.org/10.1007/s40204-018-0095-0>.

Kartini, K., Alviani, A., Anjarwati, D., Fanany, A. F., Sukweenadhi, J., & Avanti, C. (2020). Process optimization for green synthesis of silver nanoparticles using indonesian medicinal plant extracts. *Processes*, 8(8), 998. <https://doi.org/10.3390/pr8080998>.

Kong, Y.R., Jong, Y.X., Balakrishnan, M., Bok, Z.K., Weng, J.K.K., Tay, K.C., Goh, B.H., Ong, Y.S., Chan, K.G., Lee, L.H. & Khaw, K.Y., 2021. Beneficial role of *Carica papaya* extracts and phytochemicals on oxidative stress and related diseases: A mini review. *Biology*, 10(4), 287. <https://doi.org/10.3390/biology10040287>.

Kumar, B., Priyadarshi, R., Deeba, F., Kulshreshtha, A., Gaikwad, K. K., Kim, J., Kumar, A., & Negi, Y. S. (2020). Nanoporous sodium carboxymethyl

cellulose-g-poly (Sodium acrylate)/FeCl<sub>3</sub> hydrogel beads: Synthesis and characterization. *Gels*, 6(4), 49. <https://doi.org/10.3390/gels6040049>.

Kusumaningsih, T., Prasetyo, W. E., & Firdaus, M. (2020). A greatly improved procedure for the synthesis of an antibiotic-drug candidate 2, 4-diacetylphloroglucinol over silica sulphuric acid catalyst: multivariate optimisation and environmental assessment protocol comparison by metrics. *RSC Advances*, 10(53), 31824-31837. <https://doi.org/10.1039/D0RA05424K>.

Kusumaningsih, T., Prasetyo, W. E., Wibowo, F. R., & Firdaus, M. (2021). Toward an efficient and eco-friendly route for the synthesis of dimeric 2,4-diacetyl phloroglucinol and its potential as a SARS-CoV-2 main protease antagonist: insight from in silico studies. *New Journal of Chemistry*, 45(17), 7830-7843. <https://doi.org/10.1039/D0NJ06114J>.

Lavigne, J. P., Hosny, M., Dunyach-Remy, C., Boutet-Dubois, A., Schuldiner, S., Cellier, N., Martinez, A.Y., Molle, V., Scola, B.L., Marchandin, H., & Sotto, A. (2021). Long-term intrahost evolution of *Staphylococcus aureus* among diabetic patients with foot infections. *Frontiers in Microbiology*, 12, 741406. <https://doi.org/10.3389/fmicb.2021.741406>.

Lipinski, C. A., Lombardo, F., Dominy, B. W., & Feeney, P. J. (2012). Experimental and computational approaches to estimate solubility and permeability in drug discovery and development settings. *Advanced Drug Delivery Reviews*, 64, 4-17. <https://doi.org/10.1016/j.addr.2012.09.019>

Mofrad, A. S., Mohammadi, M. J., Mansoorian, H. J., Khaniabadi, Y. O., Jebeli, M. A., Khanjani, N., Khoshgoftar, M., & Yari, A. R. (2018). The antibacterial effect of g3-poly-amidoamine dendrimer on gram negative and gram positive bacteria in aqueous solutions. *Desalination and Water Treatment*, 124, 223-231. <https://doi.org/10.5004/dwt.2018.22436>.

Mulyono, L. M. (2014). Aktivitas antibakteri ekstrak etanol biji buah pepaya (*Carica papaya* L.) terhadap *Escherichia coli* dan *Staphylococcus aureus*. *Calyptra*, 2(2), 1-9.

Parani, M., Lokhande, G., Singh, A., & Gaharwar, A. K. (2016). Engineered nanomaterials for infection control and healing acute and chronic wounds. *ACS Applied Materials & Interfaces*, 8(16), 10049-10069. <https://doi.org/10.1021/acsami.6b00291>.

Parid, D. M., Abd Rahman, N. A., Baharuddin, A. S., Mohammed, M. A. P., Johari, A. M., & Razak, S. Z. A. (2018). Synthesis and characterization of carboxymethyl cellulose from oil palm empty fruit bunch stalk fibres. *BioResources*, 13(1), 535-554.

<https://doi.org/10.15376/biores.13.1.535-554>.

Prasetyo, W. E., Kusumaningsih, T., & Firdaus, M. (2019). Highly efficient and green synthesis of diacylphloroglucinol over treated natural zeolite mordenite and the optimization using response surface method (RSM). *Synthetic Communications*, 49(23), 3352-3372. <https://doi.org/10.1080/00397911.2019.1666282>.

Prasetyo, W. E., Purnomo, H., Sadrini, M., Wibowo, F. R., Firdaus, M., & Kusumaningsih, T. (2023). Identification of potential bioactive natural compounds from Indonesian medicinal plants against 3-chymotrypsin-like protease (3CLpro) of SARS-CoV-2: molecular docking, ADME/T, molecular dynamic simulations, and DFT analysis. *Journal of Biomolecular Structure and Dynamics*, 41(10), 4467-4484. <https://doi.org/10.1080/07391102.2022.2068071>.

Qi, L., Zhang, C., Wang, B., Yin, J., & Yan, S. (2022). Progress in hydrogels for skin wound repair. *Macromolecular Bioscience*, 22(7), 2100475. <https://doi.org/10.1002/mabi.202100475>.

<sup>1</sup>Singh, H. K., Patil, T., Vineeth, S. K., Das, S., Pramanik, A., & Mhaske, S. T. (2020). Isolation of microcrystalline cellulose from corn stover with emphasis on its constituents: corn cover and corn cob. *Materials Today: Proceedings*, 27, 589-594. <https://doi.org/10.1016/j.matpr.2019.12.065>

<sup>2</sup>Singh, P. G., Madhu, S. B., Shailasree, S., TS, G., Basalingappa, K. M., & BV, S. (2020). In vitro antioxidant, anti-inflammatory and anti-microbial activity of *Carica papaya* seeds. *Global Journal of Medical Research*, 20, 19-38. <https://doi.org/10.34257/GJMRBVOL20IS2PG19>.

Sofrenić, I., Andelković, B., Gođevac, D., Ivanović, S., Simić, K., Ljujić, J., Tešević, V. and Milosavljević, S. (2023). Metabolomics as a potential chemotaxonomical tool: application on the selected euphorbia species growing wild in Serbia. *Plants*, 12(2), 262. <https://doi.org/10.3390/plants12020262>.

Tuyet Phan, M. T., Pham, L. N., Nguyen, L. H., & To, L. P. (2021). Investigation on Synthesis of Hydrogel Starting from Vietnamese Pineapple Leaf Waste-Derived Carboxymethylcellulose. *Journal of Analytical Methods in Chemistry*, 2021. <https://doi.org/10.1155/2021/6639964>

Verma, A. K., & Aggarwal, R. (2021). Repurposing potential of FDA-approved and investigational drugs for COVID-19 targeting SARS-CoV-2 spike and main protease and validation by machine learning algorithm. *Chemical Biology*

& Drug Design, 97(4), 836-853. <https://doi.org/10.1111/cbdd.13812>

Wahyuni, H. S., Yuliasmi, S., Aisyah, H. S., & Riati, D. (2019). Characterization of synthesized sodium carboxymethyl cellulose with variation of solvent mixture and alkali concentration. Open Access Macedonian Journal of Medical Sciences, 7(22), 3878. <https://doi.org/10.3889/oamjms.2019.524>

Wan Ishak, W. H., Ahmad, I., Ramli, S., & Mohd Amin, M. C. I. (2018). Gamma irradiation-assisted synthesis of cellulose nanocrystal-reinforced gelatin hydrogels. Nanomaterials, 8(10), 749. <https://doi.org/10.3390/nano8100749>

Widiarto, S., Pramono, E., Rochliadi, A., & Arcana, I. M. (2019). Cellulose nanofibers preparation from cassava peels via mechanical disruption. Fibers, 7(5), 44. <https://doi.org/10.3390/fib7050044>

Yao, H., Ke, H., Zhang, X., Pan, S. J., Li, M. S., Yang, L. P., Schreckenbach, G., & Jiang, W. (2018). Molecular recognition of hydrophilic molecules in water by combining the hydrophobic effect with hydrogen bonding. Journal of the American Chemical Society, 140(41), 13466-13477. <https://doi.org/10.1021/jacs.8b09157>.

Yao, W., Weng, Y., & Catchmark, J. M. (2020). Improved cellulose X-ray diffraction analysis using Fourier series modeling. Cellulose, 27(5), 5563-5579. <https://doi.org/10.1007/s10570-020-03177-8>

Yu, J., Wang, J., Zhang, Y., Chen, G., Mao, W., Ye, Y., Kahkoska, A.R., Buse, J.B., Langer, R., & Gu, Z. (2020). Glucose-responsive insulin patch for the regulation of blood glucose in mice and minipigs. Nature Biomedical Engineering, 4(5), 499-506. <https://doi.org/10.1038/s41551-019-0508-y>

Zebua, N., Saputri, M., Sijabat, W. G., Wulandari, I. A. S. R., Nofriani, I., Zai, W. A., Arista, R.A., Suhaimi, M., & Firda, A. (2021). Incision wound healing test of ethanolic extract gel from salaon (*Parsonsia alboflavescens* [Dennst.] Mabb.) Leaves in male rats. Open Access Macedonian Journal of Medical Sciences, 9(A), 776-781. <https://orcid.org/0000-0002-4877-9960>.

Zeng, Z., Zhu, M., Chen, L., Zhang, Y., Lu, T., Deng, Y., Ma, W., Xu, J., Huang, C. & Xiong, R. (2022). Design the molecule structures to achieve functional advantages of hydrogel wound dressings: Advances and strategies. Composites Part B: Engineering, 110313. <https://doi.org/10.1016/j.compositesb.2022.110313>.

Zhang, X., Qin, M., Xu, M., Miao, F., Merzougui, C., Zhang, X., Wei, Y., Chen, W., & Huang, D. (2021). The fabrication of antibacterial hydrogels for wound healing. European Polymer Journal, 146, 110268. <https://doi.org/10.1016/j.eurpolymj.2021.110268>